J|A|C|S
ARTICLES
Published on Web 03/07/2002

Investigation on the Nature of the Adsorption Sites of Pyrrole in Alkali-Exchanged Zeolite Y by Nuclear Magnetic Resonance in Combination with Infrared Spectroscopy

Manuel Sánchez-Sánchez† and Teresa Blasco*

Contribution from the Instituto de Tecnología Química (UPV-CSIC), Avda. de los Naranjos s/n, 46022, Valencia, Spain

Received August 7, 2001. Revised Manuscript Received October 26, 2001

Abstract: Multinuclear solid-state NMR and infrared spectroscopy have been applied to investigate the host−guest interactions and the nature of the adsorption sites of pyrrole on alkali-exchanged zeolites Y (LiNaY, NaY, KNaY, and CsNaY). The presence of pyrrole provokes changes in the MAS NMR spectra of ^{23}Na, ^{7}Li, and ^{133}Cs to a degree dependent upon the amount adsorbed. The decrease in the quadrupolar coupling constant for ^{23}Na as well as the shift for ^{7}Li and ^{133}Cs signals are attributed to the interaction of the cation with the pyrrole ring system. The adsorption of pyrrole induces the displacement of cations located at SI' and SII sites toward the supercage to bind the guest molecules. In this way, the distribution of the cations at nonframework sites depends on the amount of adsorbate in the zeolite. At low loadings, pyrrole molecules bind preferentially to more electropositive cation in partially exchanged zeolites Y. Quantitative analysis by ^{1}H NMR shows that the cation−pyrrole complexes formed possess a stoichiometry of 1:1. The origin of the basic site heterogeneity, evidenced by the presence of several components in the −NH infrared stretching band, is investigated assuming that the heterocycle of pyrrole interacts with cations at SII sites in the supercage and the −NH group forms a hydrogen bond with a basic oxygen atom placed in the framework six-member ring. Making use of the information derived from NMR, it is concluded that the main source of basic site heterogeneity comes from the number of aluminum atoms in the six-member rings of the SII site where the alkaline cation is located.

Introduction

Alkali-exchanged zeolites possess basic properties which make them useful as basic catalysts in a variety of organic reactions[1,2] and as adsorbents in separation processes.[3,4] For many years, much more attention has been paid to the characterization and application of acidic zeolites, probably because of the high economical impact of acid-catalyzed petrochemical processes. However, the research activity on basic zeolites, and on heterogeneous basic catalysis in general, has experienced a growing interest in the last fifteen years.[1−4] The catalytic and sorption properties of basic zeolites will be determined by the number, strength, distribution, and accessibility of basic sites; the framework topology; and the interaction with reactants and sorbate molecules. Therefore, a deep characterization also involving the host−guests interactions is desirable to rationalize its performance as catalysts and sorbents.

Intrinsic zeolite basicity is associated with framework oxygen atoms bearing the negative charge and is thus of Lewis type. The application of the Sanderson electronegativity equalization allows facile estimation, from its chemical composition, of the average charge over the oxygen atoms.[5] An increase in the aluminum content, and for a given Si/Al ratio, a decrease of the electronegative character of the nonframework compensating cations enhance the negative charge over oxygen ions.[2,5] Therefore, the basicity of alkali-exchanged zeolites increases with the compensating cation in the order $Li^+ < Na^+ < K^+ < Rb^+ < Cs^+$.[5] These trends are also supported by applying the more sophisticated electronegativity equalization method (EEM) of calculation, which considers structure effects.[6]

The most common approach to characterize zeolite basicity involves the use of acid molecules as probes; they interact with the basic sites and the species formed are identified by the proper spectroscopic technique.[2] Among the molecules proposed as adequate probes, pyrrole (C_4H_4NH) is the most used. The proton of the −NH group interacts with the framework basic oxygen atoms forming hydrogen bridge ($C_4H_4NH\cdots O_{zeol}$) and polarizing the −NH bond. As a consequence, the infrared (IR) −NH stretching frequency shifts to lower wavenumbers as the basicity of the adsorption site increases,[5,7] showing a good correlation with the mean oxygen charge as calculated by applying the Sanderson method.[5] Similar results were found for the variation of the N_{1s} X-ray photoelectron spectroscopy (XPS) binding energy of adsorbed pyrrole[8] and more recently for the ^{1}H nuclear

* To whom correspondence should be addressed. E-mail: tblasco@itq.upv.es.
† Present address: Davy Faraday Research Laboratory, The Royal Institution of Great Britain, 21 Albemarle Street, London W1S 4BS, UK.

(1) Hattori, H. *Chem. Rev.* **1995**, *95*, 537.
(2) Barthomeuf, D. *Catal. Rev.* **1996**, *38*, 521.
(3) Corbin, D. R.; Mahler, B. A. World Patent, W. O. 94/02440, 1994.
(4) Grey, C. P.; Corbin, D. R. *J. Phys. Chem.* **1995**, *99*, 16821.
(5) Barthomeuf, D. *J. Phys. Chem.* **1984**, *88*, 42.
(6) Heidler, R.; Janssens, G. O. A.; Mortier, W. J.; Schoonheydt, R. A. *J. Phys. Chem.* **1996**, *100*, 19728.
(7) Scokart, P. O.; Rouxhet, P. G. *Bull. Soc. Chim. Belg.* **1981**, *90*, 983.

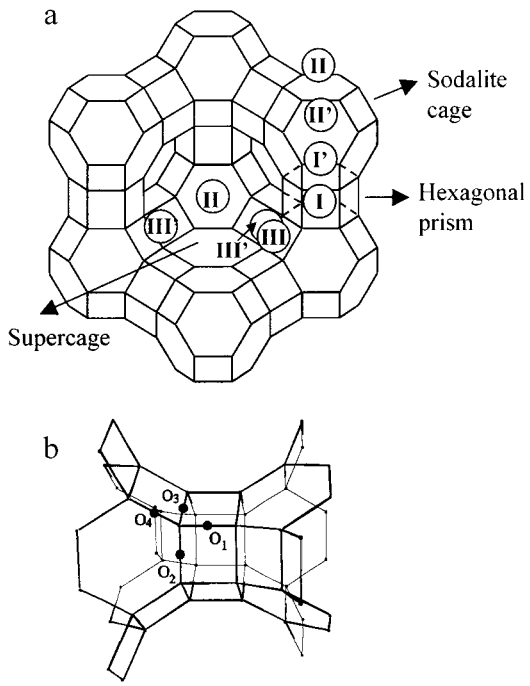

Figure 1. Schematic representation of FAU type zeolite indicating (a) the nonframework cationic sites and (b) the four nonequivalent oxygen crystallographic sites.

magnetic resonance (NMR) shift of the −NH group of pyrrole adsorbed on alkali FAU type zeolites.[9] However, pyrrole chemisorbs dissociatively on strong basic metal oxides, and in these cases, it is not a good probe molecule.[10]

The basicity in zeolites was initially interpreted as a property of the whole solid.[7] Later, the adsorption of pyrrole in various zeolites (X, Y, L, mordenite, ZSM-5) showed that the −NH frequency shift is structure-dependent and only zeolites with the same topology can be compared, which was attributed to local effects.[5] The most probable adsorption sites were assumed to be the basic oxygen atoms of the rings in the large cages where cations are placed.[5] The polarization of the adsorbed molecules will depend on the acid−base character (chemical composition and average charges) of the site and also on the dipolar moment generated by the cation−oxygen ring configuration.[5] For alkali-exchanged FAU zeolites containing two kinds of cations, the presence of two −NH stretching vibration bands and two N_{1s} XPS peaks was ascribed to pyrrole adsorbed on framework oxygen adjacent to the two kinds of alkaline cations.[8,11,12] Computer decomposition of the broad −NH stretching band of pyrrole adsorbed on alkali-exchanged zeolites EMT and FAU revealed the presence of several components corresponding to distinct basic sites defined by the nature and the location of the exchanged cations.[13,14]

Figure 1 depicts the framework structure of faujasite type zeolite, with the nonframework cation positions, and the four crystallographic oxygen atoms.[15] Sites SI are placed inside the hexagonal prisms, SI' and SII' are placed on the six-ring windows within the sodalite cage, and the SII cations are placed on the six-ring windows in the supercage. Sites SIII and SIII' are also within the supercage cavity. In alkali-exchanged zeolites Y, only sites SI, SI' and SII are usually occupied. Zeolite EMT, considered a hexagonal FAU type zeolite, possesses two nonequivalent SI (SI_a and SI_b), SI' (SI'_a and SI'_b), and SII (SII_a and SII_b) sites because of the different arrangement of the cages. From the relative intensity of the components in the IR spectra and the distribution of the cations at specific positions, the basic sites were ascribed to framework oxygen atoms adjacent to the alkaline cation at sites SI_a, SI'_b, SI'_a and SII in zeolite EMT[13] and to sites SI, SI', and SII in zeolite FAU.[14] Although pyrrole can only enter the supercages, it is assumed to have access to all oxygen atoms, including those associated with cations into the hexagonal prisms (SI) and small sodalite cages (SI').[13,14] The site heterogeneity revealed by IR indicates that the influence of cations is limited to adjacent atoms, and then basicity is determined by the local environment rather than by the bulk composition.[8,11−14] Nevertheless, the average zeolite basicity can be estimated from the mean value of the −NH stretching frequency of the IR components as supported by the improved correlation with the oxygen charge calculated by the method of Sanderson.[13]

Pyrrole is an amphoteric molecule and therefore able to interact with Lewis acid sites by donating electron from its ring system. By applying the acid−base pair concept to basic zeolites, the conjugated Lewis acid sites are the nonframework compensating cations, whose acid strength is higher at low Al content and decreases from Li^+ to Cs^+ in the alkali series.[5] Therefore, to get a complete picture of the adsorption site, the interaction of pyrrole with the cations must be considered, as first suggested by the application of the EEM and the Monte Carlo techniques to the adsorption of pyrrole over alkali zeolites of FAU type.[16] By this method, only one adsorption site with the ring interacting with the cation at sites SII and the −NH group pointing to the most basic oxygen O4 was found at low loadings.[16] A similar model but with the imino hydrogen directed toward the O1 oxygen has been proposed from quantum mechanical calculations and force field simulations.[17] Both O1 and O4 oxygen, protruding toward the supercage, were previously identified as the most basic.[6] The interaction of the ring with the cations was also suggested from inelastic neutron scattering (INS) and X-ray diffraction Rietveld refinement,[17] as well as from NMR experiments.[9,18,19] On the basis of the calculations, the interpretation of the asymmetry of the −NH IR band[13,14] was questioned, and the contribution of several components was suggested to be due to the heterogeneity of the Al distribution in six-ring tetrahedra rather than to the cation location.[16,18]

Therefore, though the use of pyrrole as an IR probe molecule is the most common method to characterize zeolite basicity,

(8) Huang, M.; Adnot, A.; Kaliaguine, S. *J. Am. Chem. Soc*. **1992**, *114*, 10005.
(9) Sánchez-Sánchez, M.; Blasco, T. *Chem. Commun*. **2000**, 491.
(10) Scokart, P. O.; Rouxhet, P. G. *J. Chem. Soc., FaradayTrans. 1* **1980**, *76*, 1476.
(11) Huang, M.; Adnot, A.; Kaliaguine, S. *J. Catal*. **1992**, *137*, 322.
(12) Huang, M.; Kaliaguine, S. *J. Chem. Soc., Faraday Trans. 1* **1992**, *88*, 751.
(13) Murphy, D.; Massiani, P.; Franck, R.; Barthomeuf, D. *J. Phys. Chem*. **1996**, *100*, 6731.
(14) Murphy, D.; Massiani, P.; Franck, R.; Barthomeuf, D. *Stud. Surf. Sci. Catal*. **1997**, *105 (Progress in Zeolite and Microporous Materials)*, 639.
(15) Mortier, W. J. *Compilation of Extraframework Sites in Zeolites*; Butterworth-Heineman: London, 1982.
(16) Heidler, R.; Janssens, G. O. A.; Mortier, W. J.; Schoonheydt, R. A. *Microporous Mater*. **1997**, *12*, 1.
(17) Förster, H.; Fuess, H.; Geidel, E.; Hunger, B.; Jobic, H.; Kirschhock, C.; Klepel, O.; Krause, K. *Phys. Chem. Chem. Phys*. **1999**, *1*, 593.
(18) Sánchez-Sánchez, M. Ph.D. Thesis, Universidad Politécnica de Valencia, Spain, 2000.
(19) Sánchez-Sánchez, M.; Blasco, T. *Stud. Surf. Sci. Catal*. **2001**, *135 (Zeolites and Mesoporous Materials at the Dawn of the 21st Century)*, 1913.

the assignment of the −NH bands is still controversial.[5,13,14,16] From the adsorption models proposed in the literature, it arises that the cation distribution in the zeolite will play an important role in the pyrrole−zeolite interaction. Statistical methods[20,21] besides X-ray powder diffraction and solid-state NMR and techniques[22−24] have shown that alkaline cations are not fixed to specific sites and that their distribution and location can be modified with the temperature of dehydration or the presence of guest molecules.[20−24] Therefore, cation migration upon pyrrole admission cannot be ignored to get a complete insight in the nature of the basic adsorption sites. In this publication, we investigate the host−guest interactions of pyrrole adsorbed over alkali-exchanged zeolite Y by the combined use of solid-state NMR and IR spectroscopies. Multinuclear solid-state NMR allows determination of the nature and location of the cations interacting with pyrrole at varying coverage and offers experimental support to give a new attribution to the different IR bands. This approach allows us to conclude that the basic site heterogeneity is mainly originated by the local composition (Si/Al ratio and the type of cation) of the adsorption site.

Experimental Section

Materials. Zeolite NaY (CBV 100, PQ zeolite) was commercially available. Zeolites LiNaY, CsNaY, and KNaY were prepared from NaY by conventional chemical exchange using 1 M aqueous solution of the corresponding alkaline chloride and refluxing at 353 K for 1 h. Two exchange processes were carried out, and after each, samples were filtered, washed until total absence of chloride, and dried at 353 K. Elemental chemical analyses were carried out by atomic absorption, and Li was measured by inductively coupled plasma spectroscopy (ICP). ^{29}Si magic angle spinning (MAS) NMR confirmed the Si/Al ratio to be 2.5 in all samples, and ^{27}Al MAS NMR showed the absence of extraframework species. The chemical composition of the zeolites, referred to the unit cell, resulted to be $Li_{34}Na_{21}Si_{137}Al_{55}O_{384}$ for LiNaY, $Na_{55}Si_{137}Al_{55}O_{384}$ for NaY, $K_{40.5}Na_{14.5}Si_{137}Al_{55}O_{384}$ for KNaY, and $Cs_{37}Na_{18}Si_{137}Al_{55}O_{384}$ for CsNaY, respectively. Prior to its use, pyrrole (>98%, supplied by Aldrich) was distilled under vacuum and the liquid was kept in the darkness to prevent its oxidation under the action of light.

Solid-State NMR. The zeolites were introduced into glass tubes and heated under dynamic vacuum at 673 K for 12 h until a final pressure below 10^{-5} kPa. The adsorption was carried out at room temperature by contacting the sample with the vapor pressure of pyrrole during 5 min, followed by degassing at increasing temperatures: 338, 423, and 473 K during 30 min. After each temperature treatment, the samples were transferred to the NMR rotors with two O-ring caps, in a glovebox in a N_2 atmosphere.

Solid-state ^{1}H, ^{7}Li, ^{23}Na, and ^{133}Cs NMR spectra were recorded at room temperature with a Varian VXR−S 400 WB spectrometer at 399.9 MHz, 155.4, 105.8, and 52.5 MHz, respectively. A 5-mm VT CP/MAS Varian probe with silicon nitride rotors and Kel-f caps with double O-ring was used to acquire the ^{1}H, ^{7}Li, and ^{23}Na spectra. The ^{133}Cs spectra were recorded with a 5-mm VT high speed Doty probe with silicon nitride rotors and macor caps with double O-ring. The samples were spun at c.a. 7 kHz and 13 kHz in the Doty and Varian probes, respectively. The proton spectra were acquired using $\pi/2$ rad pulses of 6 μs and a recycle delay of 5 s. Pulses of 1 μs corresponding to a flip angle of $\pi/8$ rad and recycle delays of 1 and 2 s were used for ^{7}Li and ^{23}Na, respectively. ^{133}Cs spectra were recorded using pulses of 0.5 μs to flip the magnetization of an angle of $\pi/24$ rad and a delay of 2 s. ^{23}Na, ^{7}Li, and ^{133}Cs chemical shifts are referenced to 0.1 M solutions of corresponding alkali chloride. Experimental spectra were simulated with the contribution of quadrupolar or Gaussian signals using the software WINFIT.

IR Spectroscopy. Fourier transformed infrared (FTIR) measurements were performed on a Nicolet 710 FT spectrophotometer with a digital resolution of 4 cm^{-1} using self-supporting wafers of 10 mg cm^{-2} and Pyrex vacuum IR cell. The samples were submitted to the same activation protocol described above, i.e., treated under dynamic vacuum at 673 K for 12 h and, after cooling at room temperature, contacted with the vapor pressure of pyrrole followed by degassing at different increasing temperatures for 30 min.

Results

In this paper, ^{23}Na as well as ^{7}Li (for LiNaY) and ^{133}Cs (for CsNaY) MAS NMR have been applied to investigate the interactions between the pyrrole molecules and the extraframework compensating cations in alkali-exchanged zeolites Y. We have studied zeolites after dehydration and upon pyrrole adsorption at room temperature and subsequent evacuation at increasing temperatures up to 473 K, starting from 338 K to eliminate the physisorbed species. Although the effect of loading can also be studied by exposing the zeolite to controlled amounts of pyrrole, we chose to increase the degassing temperature as it favors the homogeneous distribution of the adsorbate molecules in the sample and gives more direct information on the relative strength of the adsorption sites. The number of pyrrole molecules present after each treatment was estimated from the ^{1}H MAS NMR spectra. To correlate the information regarding the cation−pyrrole interaction with the heterogeneity of basic sites detected by the shift of the −NH stretching frequency, we carried out a parallel study using infrared spectroscopy.

Solid-State NMR Spectroscopy: The Cation−Pyrrole Interactions.

Zeolite NaY. Powder neutron[25] and X-ray diffraction[23] techniques show that sodium cations are located at sites SI, SI', and SII in zeolite NaY. While sites SII (multiplicity: 32/unit cell) are almost fully occupied, the fractional occupancy of positions SI (multiplicity: 16/unit cell) and SI' (multiplicity: 32/unit cell) is of c.a. 0.6 and 0.1.[23,25] Also ^{23}Na solid-state NMR spectroscopy has been applied to characterize the sodium cations and their distribution in nonframework positions in zeolites NaY and NaX.[23,24,26−29] The interaction of the nuclear quadrupole moment of ^{23}Na ($I = 3/2$, 100% naturally abundant) with the electric field gradient created by the environment leads to signals whose quadrupolar parameters strongly depend on the local site symmetry. The overlapping of several lines with different shapes results in very complex NMR spectra, which are difficult to analyze.

Na^+ at sites SI in the hexagonal prisms are characterized by a very small quadrupolar coupling constant (QCC) giving rise to an NMR signal with a comparatively narrow Gaussian line, suggesting a quite symmetric environment.[23,24,26−29] Classically, SI Na^+ cations in bare zeolite NaY were assumed to be in

(20) Van Dun, J. J.; Mortier, W. J. *J. Phys. Chem.* **1988**, *92*, 6740.
(21) Van Dum, J. J.; Dhaeze, K.; Mortier, W. J. *J. Phys. Chem.* **1988**, *92*, 6747.
(22) Norby, P.; Poshni, F. I.; Gualtieri, A. F.; Hanson, J. C.; Grey, C. P. *J. Phys. Chem. B* **1998**, *102*, 839.
(23) Grey, C. P.; Poshni, F. I.; Gualtieri, A. F.; Norby, P.; Hanson, J. C.; Corbin, D. R. *J. Am. Chem. Soc.* **1997**, *119*, 1981.
(24) Lim, K. H.; Grey, C. P. *J. Am. Chem. Soc.* **2000**, *122*, 9768.
(25) Fitch, A. N.; Jobic, H.; Renouprez, A. *J. Phys. Chem*. **1986**, *90*, 1311.
(26) Feuerstein, M.; Hunger, M.; Engelhardt, G.; Amoureux, J. P. *Solid State Nucl. Magn. Reson.* **1996**, *7*, 95.
(27) Hunger, M.; Sarv, P.; Samoson, A. *Solid State Nucl. Magn. Reson*. **1997**, *9*, 115.
(28) Hu, K.-N.; Hwang, L.-P. *Solid State Nucl. Magn. Reson*. **1998**, *12*, 211.
(29) Engelhardt, G. *Microporous Mater*. **1997**, *12*, 369.

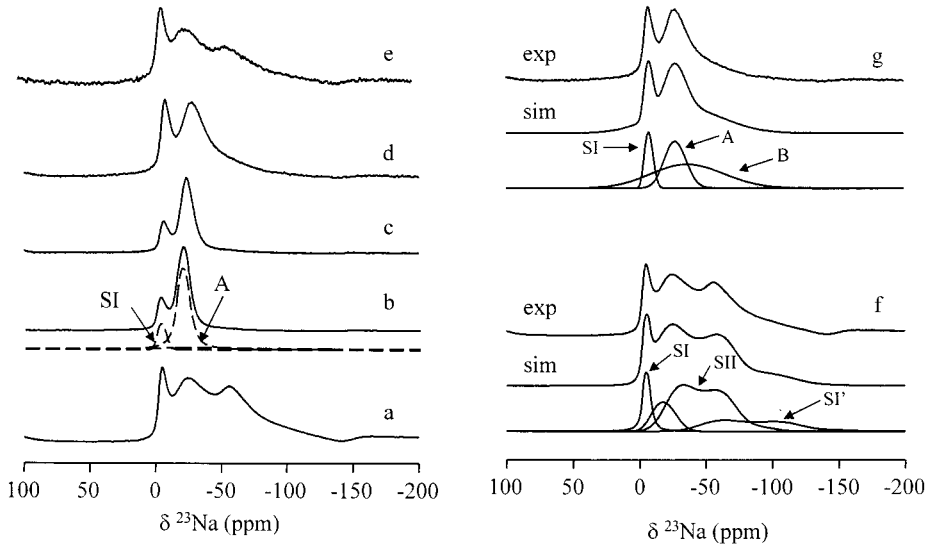

Figure 2. ^{23}Na MAS NMR spectra of zeolite NaY: (a) bare; and after the adsorption of pyrrole at room temperature and subsequent degassing at (b) 338 K, (c) 393 K, (d) 423 K, and (e) 473 K. Results of the simulation of the spectra of the zeolite NaY: (f) bare and (g) after the adsorption pyrrole at room temperature and subsequent degassing at 423 K. Dashed lines are the components of spectrum b. The intensity of the spectra is normalized.

octahedral coordination, placed at the center of the hexagonal prism.[26] However, the application of the two-dimensional (2D) multiquantum (MQ) MAS NMR technique revealed a larger QCC (1.2 MHz)[24] which was taken as evidence of the displacement of the Na^+ cations from the center of the hexagonal prism.[29] The comparatively large QCC (4.8 MHz) of Na^+ cations at the SI' positions in the sodalite cages prevented its resolution and the determination of the quadrupolar parameters in the first published 2D MQ/MAS NMR spectra of bare zeolite NaY.[27,28] Recently, this was possible with the application of high-power radio frequency pulses and fast spinning rates to record the MQ/MAS spectra.[24]

The ^{23}Na MAS NMR spectra of alkali-exchanged zeolites Y containing pyrrole molecules reported here have been simulated using the minimum number of signals which are required to get a reasonable fit and fixing the quadrupolar asymmetry parameter $\eta = 0$. We are aware that the knowledge of the exact values for the quadrupolar parameters, leading to more reliable results in the fitting of the one pulse ^{23}Na MAS NMR spectra, requires the use of field-dependent NMR experiments[26] or the most sophisticated MQ/MAS NMR technique.[24,27,28] However, the main conclusions on the Na^+−pyrrole interactions are reached considering only the sharp changes of the quadrupolar parameters, also evident from the simple comparison of the experimental spectra. The weaker point in our discussion resides on the quantification of the contributing signals when Na^+ cations are submitted to strong quadrupolar interaction. The relative intensity of the central lines in the MAS NMR spectra of noninteger quadrupolar nuclei depends on the Larmor frequency, the spinning rates, and the quadrupolar frequency,[30] and to determine the site population, the signal intensity must be corrected by applying some multiplication factor calculated by D. Massiot et al.[30] The distribution of sodium sites presented here has been calculated by correcting the intensities of the central lines.[30] At high pyrrole content, ^{23}Na signals with strong quadrupolar shapes are practically negligible leading to reliable results. At low pyrrole loading and bare Na-exchanged zeolites, the nonexact determination of the quadrupolar parameters introduces larger errors in the population of the sodium sites, since under our experimental conditions, small variation of the QCC has a strong effect on the correction factor for strong quadrupolar signals.[30] Nevertheless, the incertitude derived from the parameters extracted by the simulation of our one pulse ^{23}Na MAS NMR spectra has been considered in our discussion and does not alter the main conclusions of this work.

Figure 2a−e shows the ^{23}Na MAS NMR spectra of zeolite NaY bare and after pyrrole adsorption at 293 K and subsequent desorption at increasing temperatures. The simulation of the spectrum of the dehydrated zeolite shown in Figure 2f and the

Table 1. Results of the Simulation of the ^{23}Na MAS NMR Spectra of Zeolite NaY Dehydrated at 673 K and after the Adsorption of Pyrrole at Room Temperature and Subsequent Desorption at Increasing Temperatures (T_d)[a]

treatment	N_{py}/u.c.	Na site	N_{Na}/u.c.[b]	QCC (MHz)	δ_{iso} ^{23}Na (ppm)
dehydration	0	SI	3.0	1.2	−1.8
at 673 K		SI'	20	4.8	−33.0
		SII	28.5	4.0	−11.5
		SIII'	3.5	2.3	−6.6
T_d (pyrrole desorption)					
338 K	43	SI	7.0	1.5	1.0
		A	43	1.5	−14.7
		B	5.0	3.6	−6.8
393 K	38	SI	6.5	1.4	−2.3
		A	39	1.5	−18.6
		B	9.5	3.6	−10.1
423 K	19	SI	6.0	1.4	−9.9
		A	13	1.8	−19.8
		B	36	3.5	−9.9
473 K	0	SI	4.0	1.2	−5.7
		SI'	13.5	4.8	−34.9
		SII	31	4.0	−15.3
		SIII'	6.5	2.3	−12.6

[a] A value of $\eta = 0$ was used in the simulation of the quadrupolar signals. The number of pyrrole molecules per unit cell (N_{py}/u.c.) has been estimated from the ^{1}H NMR spectra (accuracy ±10%). [b] The Na populations are given with an accuracy of a ±5% in the bare zeolite and after the desorption of pyrrole at 338 and 393 K, and with an accuracy of ±10% after the desorption at 423 and 473 K.

(30) Massiot, D.; Bessada, C.; Coutures, J. P.; Taulelle, F. *J. Magn. Reson.* **1990**, *90*, 231.

resulting cation distribution indicated in Table 1 were obtained using the quadrupolar parameters recently determined by MQ/MAS.[24] The site population is in good agreement with those reported for a zeolite NaY of similar composition.[24] A signal previously attributed to some hydrated Na^+ sites[24] is also present in our spectrum (see unlabeled peak in Figure 2f). However, since no proton resonance of water is detected in our sample, we believe that this resonance can be produced by some sodium atoms located at SIII or SIII' supercage positions, as supported by its chemical shift and QCC value (see Table 1), close to those of a SIII' Na^+ cation in zeolite NaX.[26] After the adsorption of pyrrole and evacuation at 338 K, the zeolite NaY contains 43 molecules per unit cell (from ^{1}H NMR), that is, around five per supercage, which provokes dramatic changes in the ^{23}Na MAS NMR spectrum as shown in Figure 2b. While the Na^+ SI component remains unchanged, the quadrupolar patterns characteristic of Na^+ at sites SI' and SII disappear and the high field region of the spectrum becomes considerably narrower. As shown in Figure 2g, the spectrum consists of the SI resonance and two new components which have been denoted as A and B. Signal A, which dominates the spectrum at high loading (see spectrum 2b), possesses a small QCC value suggesting a symmetric environment. The QCC of the component B is considerably larger (3.6 MHz) and close to those of SI' and SII in the bare zeolite NaY and therefore this component is attributed to Na^+ cations which do not interact with pyrrole molecules. As the degassing temperature progressively increases, the number of adsorbed pyrrole molecules and the relative contribution of signal A decrease (see Figure 2 and Table 1), and after evacuating at 473 K, the original ^{23}Na MAS NMR spectrum of the bare zeolite NaY is practically recovered (Figure 2, Table 1).

Changes in the ^{23}Na MAS NMR spectra qualitatively analogous to those described in Figure 2 and Table 1 have been previously reported upon adsorption of chloroform[31,32] and hydrofluorocarbons (HFC)[23,24] over zeolite NaY. The absence of a signal with a quadrupolar coupling constant of the same order than the SI' in the bare zeolite NaY (not accessible to the guest molecules) was initially explained by two different postulates: (i) the migration of SI' Na^+ cations to the supercage to interact with the HFC molecules[23] and (ii) the redistribution of charges in the zeolite framework as a consequence of the hydrogen bonding with the HFC.[31] Very recently, the two hypotheses have been carefully analyzed, and the reported results support the theory of sodium migration.[24] A similar interpretation can be given to our results. The disappearance of the signal originated by Na^+ at sites SI' in the spectra of zeolite NaY containing pyrrole (see Figure 2) can be explained by their migration to the supercage.

By analogy with a new ^{23}Na resonance (QCC value smaller than those of sites SI' and SII) in NaY loaded with HFC,[24] signal A is attributed to supercage Na^+ cations interacting with pyrrole molecules. Recently, we assigned a high field shifted ^{7}Li MAS NMR peak in LiNaY containing pyrrole to the Li cations interacting with the π electrons of the pyrrole ring system.[9,19] A similar model for Na^+ cations is suggested from XRD data[17] and is further supported by theoretical calculations in the pyrrole−zeolite NaY system at low loading, which predicts the interaction of one pyrrole molecule with one Na^+ cation located in the supercage site SII.[16,17] Within the experimental error in the simulation of our ^{23}Na MAS NMR spectra, the population of Na^+ cation giving rise to signal A is close to the number of adsorbed pyrrole molecules, strongly supporting the 1:1 stoichiometry of the Na^+−pyrrole complex formed. However, from our results we cannot locate the supercage Na^+ cations at specific sites. At high loadings, the number of pyrrole−Na^+ species (signal A) is higher than the number of SII sites (32 per unit cell), and therefore pyrrole will not only interact with Na^+ at SII positions. After the evacuation at 423 K, the number of pyrrole molecules and signal A decrease while signal B increases. The larger quadrupolar coupling constant value of resonance B suggests its assignment to Na^+ cations with a very weak or no interaction with the adsorbate molecules. The quadrupolar parameters of signal B are closer to those of SII than of SI' Na^+ cations, which could suggest that they are placed in the supercage rather than in the sodalite units, even they do not bind to pyrrole. Alternatively, it could be assigned to SI' Na^+ cations which have modified its quadrupolar parameters because of framework modifications provoked by the presence of pyrrole.

For the HFC−NaY system, it was reported that some Na^+ at SI' also migrates to SI sites.[24] A similar process cannot be assessed from our data since the variation in the SI site population with the pyrrole loading is within the experimental error because of its relatively low occupancy. Finally, from the simulation of the ^{23}Na spectrum acquired after desorption at 473 K (Table 1), we think the cation distribution of the bare zeolite NaY is not completely recovered. Probably some supercage Na^+ cations, which were located into the sodalite units before the adsorption, do not migrate to their original positions when pyrrole is removed.

To summarize, we can conclude that the adsorption of pyrrole over zeolite NaY results in the migration of Na^+ from sites SI' in the sodalite cage to the supercage to bind pyrrole molecules, and we suggest that there, one pyrrole molecule interacts with one Na^+ cation.

Zeolite LiNaY. The capacity of fully exchanged zeolites X to selectively adsorb N_2 and its potential application to separate air components have been incentives to investigate the cation distribution in LiX by using neutron diffraction[33,34] and solid-state NMR[35−37] techniques. Also, some publications have been devoted to characterize partially exchanged LiNaX,[38−42] and to lesser extent, LiNaY zeolites.[9,38,39] The reported results lead to the conclusion that in Li^+ exchanged zeolites of type FAU, Li^+

(31) Bosch, E.; Huber, S.; Weitkamp, J.; Knözinger, H. *Phys. Chem. Chem. Phys.* **1999**, *1*, 579.
(32) Sánchez-Sánchez, M.; Blasco, T.; Rey, F. *Phys. Chem. Chem. Phys.* **1999**, *1*, 4529.
(33) Feuerstein, M.; Lobo, R. F. *Chem. Mater.* **1998**, *10*, 2197.
(34) Plévert, J.; Di Renzo, F.; Fajula, F.; Chiari, G. *J. Phys. Chem. B* **1997**, *101* 10340.
(35) Plévert, J.; De Menorval, L. C.; Di Renzo, F.; Fajula, F. *J. Phys. Chem. B* **1998**, *102*, 3412.
(36) Feuerstein, M.; Lobo, R. F. *Chem. Commun.* **1998**, 1647.
(37) Feuerstein, M.; Accardi, R. J.; Lobo, R. F. *J. Phys. Chem. B* **2000**, *104*, 10282.
(38) Herden, H.; Einicke, W. D.; Schöllner, R.; Mortier, W. J.; Gellens, L. R.; Uytterhoeven, J. B. *Zeolites* **1982**, *2*, 131.
(39) Forano, C.; Slade, R. C. T.; Krogh Andersen, E.; Krogh Andersen, I. G.; Prince, E. *J. Solid State Chem.* **1989**, *82*, 95.
(40) Shepelev, Y. F.; Anderson, A. A.; Smolin, Y. I. *Zeolites* **1990**, *10*, 61.
(41) Feuerstein, M.; Engelhardt, G.; McDaniel, P. L.; MacDougall, J. E.; Gaffney, T. R. *Microporous Mesoporous Mater.* **1998**, *26*, 27.
(42) Plévert, J.; Di Renzo, F.; Fajula, F.; Chiari, G. In *Proceedings of the 12th International Zeolite Conference*; Treacy, M. M. J., Marcus, B. K., Bisher, M. E., Higgins, J. B., Eds.; Materials Research Society: Warrendale, Pennsylvania, 1999; Vol. I, p 135.

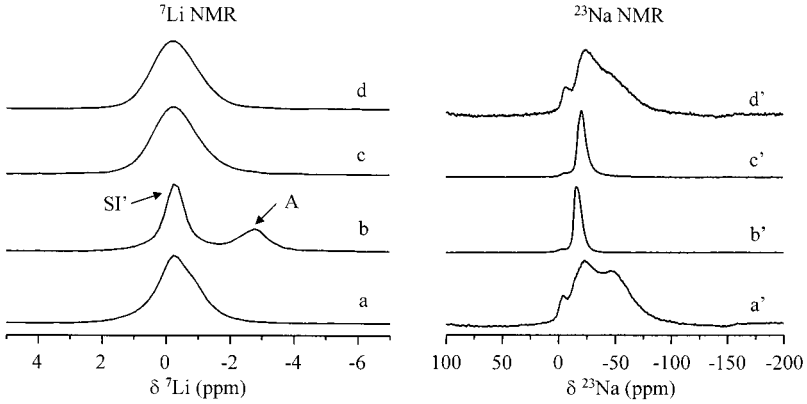

Figure 3. ^{7}Li (a−d) and ^{23}Na (a'−d') MAS NMR spectra of zeolite LiNaY: (a), (a') bare; and after the adsorption of pyrrole at room temperature and subsequent degassing at (b), (b') 338 K; (c), (c') 423 K; and (d), (d') 473 K. The intensity of the spectra is normalized.

cations prefer sites SI' and SII, located in front of the six-ring windows, and sites SIII and SIII' become occupied only at high lithium contents.[33,34,38−41]

The two natural Li isotopes, ^{6}Li (7.4% abundant) and ^{7}Li (92.6% abundant) are active in NMR. ^{7}Li possesses a nuclear spin $I = 3/2$ with a small quadrupole moment, giving NMR peaks only slightly broadened by second-order quadrupolar interaction, whereas ^{6}Li with a nuclear spin $I = 1$ possesses an even smaller quadrupole moment usually leading to better resolved spectra[33,35−37,43] but presents the disadvantage of lower natural abundance and longer relaxation times.[43] Up to three lines are observed in the ^{7}Li (and the ^{6}Li) MAS NMR spectra of Li^+ exchanged zeolite X at δ_{iso}= 0.4, −0.3, and −0.7 ppm attributed to lithium cations at sites SI', SII, and SIII, respectively.[33,35−37,40,43] A method based on the paramagnetic effect of physisorbed molecular oxygen on the chemical shift of accessible lithium cations has been proposed to discriminate different extraframework sites.[35−37] The presence of oxygen provokes a low field shift of the SIII peak in the ^{6}Li and ^{7}Li spectra of Li^+ exchanged zeolites X reflecting its interaction with these paramagnetic gas molecules.[35−37] Also, the adsorption of N_2 has been reported to cause a slight high field shift (0.2 ppm) of the resonance of Li^+ at SIII positions, which allows to determine the cations directly involved in the N_2 adsorption process.[36,37] Oxygen and nitrogen molecules can only enter the supercage in faujasite type zeolites and then cations at site SI' into the sodalite units are not accessible. Although sites II are located in the supercage, Li^+ cations are inside the six-ring window and are shielded by the oxygen atoms, preventing its contact with the gas molecules, which explains the absence of interaction.[35−37]

Figure 3a shows the ^{7}Li MAS NMR spectrum of dehydrated zeolite LiNaY. The spectra recorded under vacuum and in the presence of N_2 consist of an asymmetric line that can be simulated by two components at −0.1 and at c.a. −0.7 ppm, but the resolution is not enough to determine if the adsorption of N_2 shifts the position of the shoulder. Although the chemical shifts do not coincide with those previously reported for LiX zeolites, we attribute the main resonance at −0.1 ppm to SI' Li^+ and the shoulder to SII Li^+ cations. This assignment is based on the relative signal intensity and the preference of Li for site SI',[38−41] besides the reported high field shift for the ^{7}Li SII resonance.[33,36,37,41] The relatively low Li content, insufficient to complete SI' and SII positions (64/u.c.), explains the absence of a signal of SIII sites.[38−41]

When pyrrole is adsorbed and the sample evacuated at 338 K, a high field shifted peak appears and the main signal becomes symmetric, indicating the interaction of pyrrole molecules with Li^+ originally at sites SII (see Figure 3b), which are not accessible to N_2 and O_2 in zeolites X. The O−Li−O bond angles reported for Li exchanged zeolites X and Y are quite similar[39] and suggests that Li^+ at SII sites in zeolite LiY must not be accessible to gas molecules. Therefore, upon adsorption, the SII Li^+ cations may move out of the plane of oxygens or migrate to SIII (or SIII') sites[24] to bind the pyrrole molecules. As we have previously proposed,[9] the high field shift observed upon pyrrole adsorption can be explained by the interaction of the π electrons of the pyrrole ring, which has aromatic character, with the Li^+. This interpretation is supported on the theoretical calculation of the ^{7}Li chemical shift of Li−benzene model compounds and the ^{7}Li MAS NMR spectra of LiZSM-5 containing benzene.[44] When the degassing temperature is increased to 423 K, the shifted resonance disappears and only a broad component is observed in the spectra, which suggests that pyrrole interacting with lithium cations has been desorbed (see Figure 3b−d). No ^{7}Li NMR signal is shifted when pyrrole is adsorbed over zeolite LiNaX indicating that Li^+ stay at the plane of the six-member ring.[19]

Figure 3a'−d' show the ^{23}Na MAS NMR spectra of zeolite LiNaY bare and after pyrrole adsorption and subsequent evacuation at increasing temperatures. The results of the spectra simulation are summarized in Table 2 and illustrated in Figure 4 for the zeolite bare and after the pyrrole desorption at 338 K. The spectrum of the LiNaY sample was simulated using the three signals of Na^+ at sites SI, SI', and SII (see Table 2). The quadrupolar parameters have been determined from the simulation of the one-pulse spectrum, as shown in Figure 4, and the site distribution of Na^+ cations shown in Table 2 for the bare zeolite may be affected by some error. However, our results agree with preferential site occupancy reported for Li exchanged zeolites X and Y.[33,34,38−41] As can be observed in Figure 3a'−d', the presence of pyrrole produces changes in the ^{23}Na MAS NMR spectra, similar to those described for zeolite NaY. While the SI signal is not modified, the two components with large quadrupolar interactions due to Na^+ cations at positions SI' and

(43) Feuerstein, M.; Lobo, R. F. *Solid State Ionics* **1999**, *118*, 135.

(44) Barich, D. H.; Xu, T.; Zhang, J.; Haw, J. F. *Angew. Chem., Int. Ed.* **1998**, *37*, 2530.

Table 2. Results of the Simulation of the ^{7}Li and ^{23}Na MAS NMR Spectra of Zeolite LiNaY Dehydrated at 673 K and after the Adsorption of Pyrrole at Room Temperature and Subsequent Desorption at Increasing Temperatures (T_d)[a]

treatment	N_{py}/u.c.	Li site	N_{Li}/u.c.	δ_{iso} ^{7}Li (ppm)	Na site	N_{Na}/u.c.[b]	QCC (MHz)	δ_{iso} ^{23}Na (ppm)
dehydration at 673 K	0	SI'	n.d.[c]	−0.1	SI	0.5	1.3	−0.1
		SII	n.d.	−0.7	SI'	7.5	4.2	−6.7
					SII	13	3.8	−3.0
T_d (pyrrole desorption)								
338 K	27	SI'	23.5	−0.3	SI	1.0	1.0	0.5
		A	10.5	−2.8	A	5.0	1.2	−13.3
					A'	15.0	1.6	−12.3
423 K	19	SI' SII	34	−0.3	SI	1.0	1.0	−4.0
					A	9.5	1.4	−16.5
					A'	10.5	1.9	−15.6
473 K	0.3	SI' SII	34	−0.3	SI	0.5	1.2	−2.7
					SI'	5.5	3.8	−9.3
					SII	13	4.4	−6.2
					SIII'	2.0	2.2	−15.8

[a] A value of $\eta = 0$ was used in the simulation of the quadrupolar signals. The number of pyrrole molecules per unit cell (N_{py}/u.c.) has been estimated from the ^{1}H NMR spectra (accuracy ±10%). [b] The Na populations are given with an accuracy of ±10% in the bare zeolite and after the desorption of pyrrole at 473 K and of ±5% after the desorption of pyrrole at 338 K and 423 K. [c] n.d.: not determined.

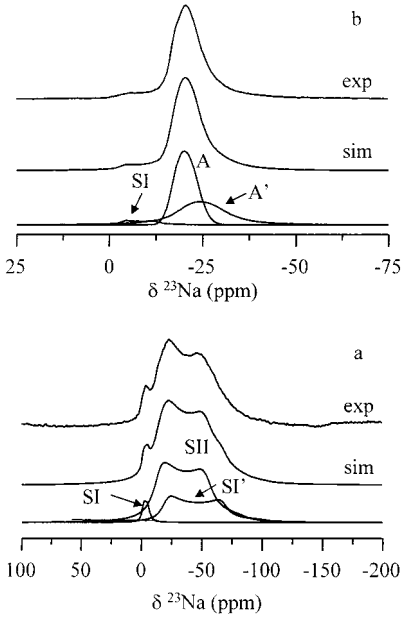

Figure 4. Results of the simulation of the ^{23}Na MAS NMR spectra of zeolite LiNaY: (A) bare and (B) after the adsorption pyrrole at room temperature and subsequent degassing at 423 K. The intensity of the spectra is normalized.

SII disappear (Figures 3 and 4). The spectrum is narrower and can be considered as formed by three components, one due to SI sites and two new signals with relatively small QCC, denoted as A and A' by their similitude with the resonance A in pyrrole containing zeolite NaY (Figure 4b). Consistently, they must be due to Na^+ interacting with the adsorbed molecules, probably through the electron density of the pyrrole cycle. As for zeolite NaY, the adsorption of pyrrole over zeolite LiNaY favors the migration of SI' Na^+ cations from the sodalite units to the supercage. This conclusion can be reached even if the population of sites SI' and SII proposed in Table 2 for the bare zeolite would be inverted because of the incertitude in the determination of the quadrupolar parameters. The diminution of the number of pyrrole molecules by raising the desorption temperature to 423 K produces only slight changes (see Figure 3c'), and only after evacuating at 473 K, the spectrum recovers its original appearance, although it is not identical to that of the bare zeolite. This suggests that the migration processes involved in the adsorption−desorption of pyrrole are not completely reversible. Nevertheless there is residual amounts of pyrrole and from our data we cannot asseverate if the original cation distribution (both Li^+ and Na^+) in the bare LiNaY zeolite has changed.

When we compare the evolution of the ^{7}Li and ^{23}Na MAS NMR spectra of zeolite LiNaY containing pyrrole with the degassing temperature, it is evident that the molecules are first desorbed from the sites associated to Li^+. The number of adsorbed pyrrole molecules after the evacuation at 338 K is 27, which is approximately the number of affected Li^+ (10 per unit cell) and Na^+ (20 per unit cell), as deduced from our NMR results. The same is observed after the evacuation at 423 K; the amount of pyrrole in the zeolite is very close to the number of Na^+ producing signals A plus A'. As for zeolite NaY, this suggests that one pyrrole molecule interacts with one cation. We must notice that the adsorption of pyrrole provokes the migration of SI' Na^+ to the supercage but not of SI' Li^+ cations. Only Li^+ at SII sites in the supercage moves from its original position to bind the pyrrole molecules.

Zeolite KNaY. Potassium isotopes are not very usual nuclei for NMR investigation because of their properties (low gyromagnetic ratio and sensitivity). For this reason, we shall only study the interaction of pyrrole with Na^+ cations in zeolite KNaY. Up to our knowledge, the distribution of Na^+ and K^+ in partially exchanged Y-type zeolites has not been reported. The application of X-ray powder methods to study dehydrated fully exchanged KY zeolites show that K^+ cations are located in sites SI, SI', and SII.[45]

Figure 5 shows the evolution of the ^{23}Na MAS NMR spectra of zeolite KNaY with the pyrrole loading. The spectrum of the bare zeolite (Figure 5a) can be simulated using three quadrupolar signals, which can be attributed to Na^+ at sites SI, SI', and SII as depicted in Figure 5e. The lack of information on the cation distribution in zeolites of type FAU of analogous composition prevents to contrast our simulation results. After the desorption of pyrrole at 338 K, the ^{23}Na spectrum becomes much more symmetric and can be decomposed in two signals, one of SI Na^+ sites and another one, denoted as A, with a low quadrupole coupling constant, as shown in Table 3. Consistent with the results for zeolites LiNaY and NaY, resonance A is assigned to supercage Na^+ cations bonded to the pyrrole molecules. Again, the spectra 5a and 5b strongly suggest that Na^+ migrates from sodalite SI' positions toward the supercage. As the amount of pyrrole progresively diminishes by increasing the degassing temperature to 423 K (see Table 3), a signal of Na^+ submitted to large quadrupole interactions emerges, probably of SI' sites, as it is evident from the simulation shown in Figure 5f and the quadrupolar parameters listed in Table 3. The degassing at 473 K practically restores the ^{23}Na NMR spectrum of the bare zeolite, even though twelve pyrrole molecules remain adsorbed (see Table 3), which strongly suggest that they must be bonded to potasium cations. The cation distributions derived from the

(45) Mortier, W. J.; Bosmans, H. J.; Uytterhoeven, J. B. *J. Phys. Chem.* **1972**, *76*, 650.

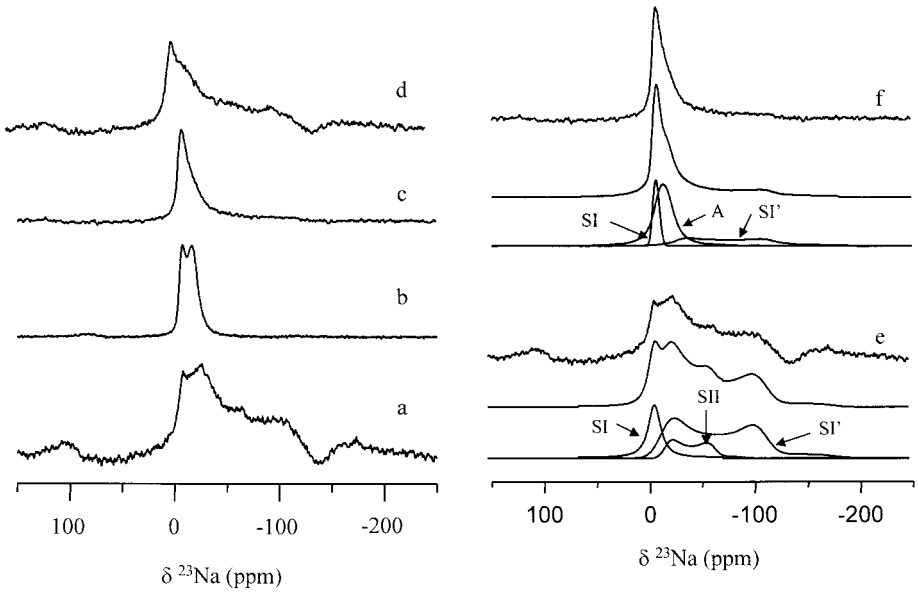

Figure 5. ^{23}Na MAS NMR spectra of zeolite KNaY: (a) bare; and after the adsorption of pyrrole at room temperature and subsequent degassing at (b) 338 K, (c) 423 K, and (d) 473 K. Results of the simulation of the spectra of the zeolite: (e) bare; and (f) after the adsorption of pyrrole at room temperature and subsequent degassing at 423 K. The intensity of the spectra is normalized.

Table 3. Results of the Simulation of the ^{23}Na MAS NMR Spectra of Zeolite KNaY Dehydrated at 673 K and after the Adsorption of Pyrrole at Room Temperature and Subsequent Desorption at Increasing Temperatures (T_d)[a]

treatment	N_{py}/u.c.	Na site	N_{Na}/u.c.[b]	QCC (MHz)	δ_{iso} ^{23}Na (ppm)
dehydration	0	SI	0.5	1.5	−6.8
at 673 K		SI'	13.5	5.7	0.9
		SII	1.0	4.0	−10.0
T_d (pyrrole desorption)					
338 K	50	SI	3.0	1.2	−4.6
		A	12.0	1.6	−11.6
423 K	38	SI	1.0	1.3	−2.7
		SI'	11	5.8	−5.2
		A	3.0	1.6	−15.2
473 K	12	SI	1.0	1.3	−3.6
		A	0.5	2.0	−10.4
		SI'	13.0	5.7	−2
		SII	1.0	4.2	−10.7
523 K	0	SI	0.5	1.3	−4.9
		SI'	13.5	6.0	8.9
		SII	1.0	4.1	−10.6

[a] A value of $\eta = 0$ was used in the simulation of the quadrupolar signals. The number of pyrrole molecules per unit cell (N_{py}/u.c.) has been estimated from the ^{1}H NMR spectra (accuracy ±10%). [b] The Na populations are given with an accuracy of ±5% after the desorption of pyrrole at 338 K and of ±10% in the bare zeolite and after the desorption at 423, 473 and 523 K.

simulation of the spectra, summarized in Table 3, show that the ratio between the number of adsorbed pyrrole molecules and of affected Na^+ increases with the desorption temperature. Although the stoichiometry of the pyrrole−cation complex formed cannot be estimated here, this observation suggests that at low loadings, pyrrole is preferentially adsorbed over more electropositive K^+ cations.

Zeolite CsNaY. ^{133}Cs is 100% naturally abundant and possesses a noninteger nuclear spin ($I = 7/2$). Its QCC is usually very small and the effect of the second-order quadrupolar interactions in the line shapes is negligible.[46,47] Although it is not clearly established,[22] field-dependent MAS NMR experiments suggest that the origin of the spinning sidebands is the chemical shift anisotropy rather than satellite transition effects.[46] The ^{133}Cs nucleus presents a very large chemical shift range, and its high sensitivity to the local environment renders the assignment of the different resonances to specific cation sites in zeolites difficult.

Previous studies on X-ray powder diffraction in combination with solid-state NMR on CsNaY led to the conclusion that after the ion exchange process, only supercage Na^+ occupying SII and SIII sites in NaY are exchanged by Cs^+.[22] Subsequent dehydration of the zeolite provokes cation migrations leading to significant changes in the site population with the evacuation temperature.[22,47] The cation mobility in the supercages increases with the temperature, resulting in the coalescence of the corresponding resonances, suggesting low energetic barriers for different cations arrangements.[22,48]

Despite some discrepancies in the interpretation of the ^{133}Cs MAS NMR spectra of zeolite CsNaY, the high field signals (in the range from −130 to −160 ppm) are generally attributed to Cs^+ within the sodalite cages, and the low field resonances are generally attributed to Cs^+ in the supercage.[22,46,49] These assignments are based on the shift suffered by the high-frequency components upon adsorption of guest molecules[22,46] and its coalescence at high temperatures.[22] However, the presence of Cs^+ cations at site SI within the hexagonal prism shown by Rietveld refinement led to the assignment of the high field signal at −153 ppm to Cs^+ at site SI and a resonance at −78 ppm (in the low field region) to Cs^+ at the SI' sodalite site.[47] The entrance of Cs^+ within the hexagonal prism has been later questioned because of the large size of this cation.[22] Figure 6a shows the ^{133}Cs MAS NMR spectrum of the dehydrated zeolite CsNaY, which is characterized by several lines with spinning sidebands. The results of its decomposition using individual Gaussian lines are shown in Figure 6e. The peak at

(46) Malek, A.; Ozin, G. A.; Macdonald, P. M. *J. Phys. Chem.* **1996**, *100*, 16662.
(47) Koller, H.; Burger, B.; Schneider, A. M.; Engelhardt, G.; Weitkamp, J. *Microporous Mater.* **1995**, *5*, 219.
(48) Hunger, M.; Schenk, U.; Buchholz, A. *J. Phys. Chem. B* **2000**, *104*, 12230.
(49) Hunger, M.; Schenk, U.; Weitkamp, J. *J. Mol. Catal. A: Chem.* **1998**, *134*, 97.

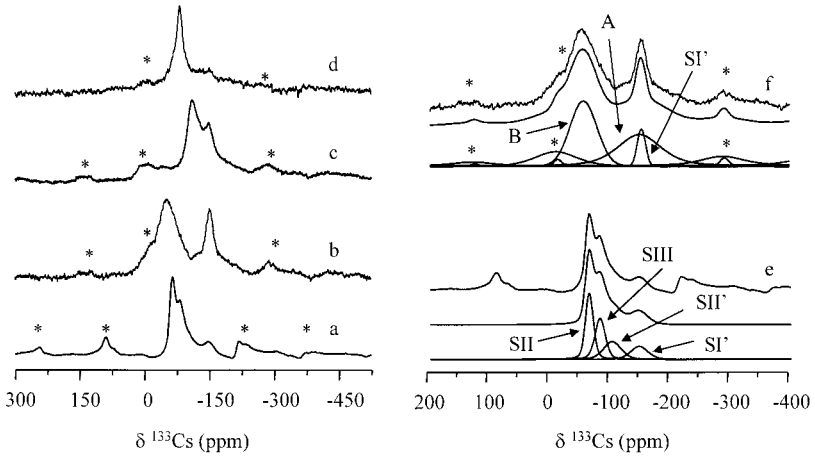

Figure 6. ^{133}Cs MAS NMR spectra of zeolite CsNaY: (a) bare; and after the adsorption of pyrrole at room temperature and subsequent degassing at (b) 338 K, (c) 423 K, and (d) 473 K. Results of the simulation of the spectra of the zeolite: (e) bare; and (f) after the adsorption of pyrrole at room temperature and subsequent degassing at 338 K. The intensity of the spectra is normalized.

Table 4. Results of the Simulation of the ^{133}Cs and ^{23}Na MAS NMR Spectra of Zeolite CsNaY Dehydrated at 673 K and after the Adsorption of Pyrrole at Room Temperature and Subsequent Desorption at Increasing Temperatures (T_d)[a]

treatment	N_{py}/u.c.	Cs site	N_{Cs}/u.c.[b]	δ_{iso} ^{133}Cs (ppm)	Na site	N_{Na}/u.c.[b]	QCC (MHz)	δ_{iso} ^{23}Na (ppm)
dehydration	0	SI'	5.5	−147	SI	6.0	1.2	−1.8
at 673 K		SII'	8.0	−102	SI', SII	12.5	5.9	21.1
		SIII	10.5	−82				
		SII	13	−64				
T_d (pyrrole desorption)								
338 K	35	SI'	4.0	−152	SI	8.0	1.2	1.7
		A	21.5	−153	A	10.5	2.1	−2.1
		B	11.5	−56				
423 K	24	SI'	7.5	−145	SI	5.5	1.1	−1.3
		A	19	−176	A	3.0	2.1	−1.6
		B	10.5	−110	SI', SII	10.0	4.6	−6.9
473 K	0.7	SI'	13.5	−147	SI	5.0	1.6	−1.6
		SII'	7.5	−102	SI', SII	13.5	4.3	−3.2
		SIII	7.5	−82				
		SII	8.5	−64				

[a] A value of $\eta = 0$ was used in the simulation of the quadrupolar signals. The number of pyrrole molecules per unit cell (N_{py}/u.c.) has been estimated from the ^{1}H NMR spectra (accuracy ±10%). [b] The Na and Cs populations are given with an accuracy of ±10%.

−147 ppm is assigned to Cs^+ within the sodalite units, probably at sites SI',[22,46,49] and the signal at −64 ppm is assigned to Cs^+ at sites SII.[22,46−49] The intermediate peaks at −82 and −102 ppm can be ascribed to sites SIII and SII', respectively.[22,46,49] The attribution of the signals and the relative site population in the bare zeolite are described in Table 4.

The ^{133}Cs MAS NMR spectra of pyrrole-loaded zeolite are shown in Figure 6 a−d, and the assignment and relative population of the signals are described in Table 4. The ^{133}Cs NMR peak of SI' sodalite cations is hardly modified by the adsorption, while the position and shape of the other signals depend on the pyrrole content (see Figure 6). The best fit of the spectrum acquired after degassing at 338 K is shown in Figure 6f. Besides the signal SI', the spectrum consists of two bands, A and B, shifted to high and low field, respectively, with respect to the main signals in the bare zeolite. Both resonances are broad, but only species A gives spinning sidebands indicating a lower mobility of Cs^+. By analogy with the high field ^{7}Li NMR signal observed after the adsorption of pyrrole over LiNaY, signal A can be tentatively attributed to a Cs^+ cation interacting with the ring of pyrrole. Assuming that one pyrrole molecule is adsorbed over one cation in zeolites Y, as deduced for NaY and LiNaY, the assignment of signal A to a Cs^+−pyrrole complex is further supported by the signal's intensities. The number of Na^+ (^{23}Na signal A, vide infra) and Cs^+ cations forming complexes must be equal to the number of adsorbed pyrrole molecules. This is true for ^{133}Cs signal A but not when signal B is considered. After adsorbing toluene over CsNaY, the appearance of a broad band shifted to low field was explained by the formation of rigidly bound adsorbate complex.[49] However, unlike our signal B, this band has several orders of spinning sidebands, and this is why we believe that must correspond to a different type of species. The Cs^+ cations giving signal B are deshielded in an environment with a lower electron density than in the bare zeolite.

Degassing at 423 K (see Figure 6c and Table 1) provokes the desorption of around 10 molecules of pyrrole bonded to Na^+ cations (^{23}Na signal A, vide infra) and a high field shift of signal B, while the Cs^+−pyrrole complex (^{133}Cs signal A) remains almost the same. The chemical shift of signal B strongly depends on the loading, and although its attribution is not completely clear for us at the moment, it must be originated by the influence of the adsorbed pyrrole, which is forming Na^+−pyrrole and Cs^+−pyrrole complexes (^{23}Na and ^{133}Cs signals A). To figure out this, it must be considered that, although to much lesser extent than alkali-exchanged zeolites X, zeolite CsNaY presents a relatively high cation population in the supercage and in the occupancy of SIII sites by voluminous Cs^+ cations. Theoretical calculation on the adsorption of pyrrole over NaX zeolites showed that SIII cations have an influence on the pyrrole −NH bond, small when compared with SII sites.[16] In the adsorption model previously proposed for zeolite NaY,[17] the pyrrole nitrogen atom is located near the SIII position, which is occupied in zeolite NaX, where the coordination of pyrrole is more complex.[17] Although it is speculative, these observations[16,17] point to some interaction between the SIII Cs^+ and the pyrrole forming complexes with the SII cations, which could originate the ^{133}Cs signal B. The disappearance of the signal attributed to SII' ^{133}Cs upon the adsorption of pyrrole suggests the migration of cesium from the sodalite to the supercage. Although the desorption at 473 K practically removes all pyrrole molecules, the ^{133}Cs spectrum of the bare zeolite is not

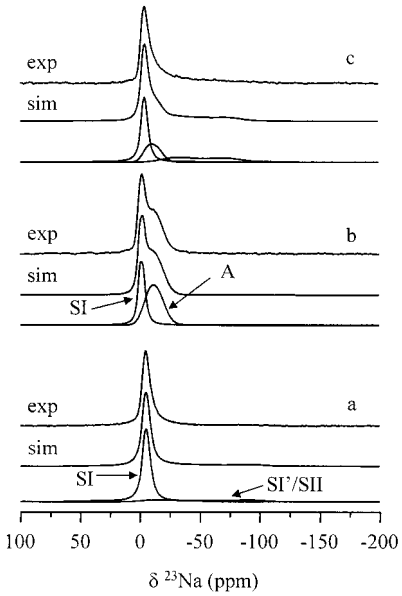

Figure 7. Results of the simulation of the ^{23}Na MAS NMR spectra of zeolite CsNaY: (a) bare; and after the adsorption of pyrrole at room temperature and subsequent evacuation at (b) 338 K and (c) 423 K. The intensity of the spectra is normalized.

completely recovered and the original site distribution, especially in the supercages, changes.

Figure 7 shows the ^{23}Na NMR spectra of sample CsNaY. The empty zeolite gives a narrow signal typical of SI cations and a component with a large QCC, which can be attributed to Na^+ at SI' or SII sites.[22,47] As it is shown in Figure 7b−c, when pyrrole is adsorbed, a new signal A appears, whose intensity decreases as pyrrole is desorbed. Again, this signal can be ascribed to Na^+−pyrrole complexes. The QCC value of ^{23}Na signal A in this sample is slightly higher than that measured for the three other zeolites included in Tables 1−3. The ^{23}Na spectrum of the bare zeolite is recovered after degassing at 473 K (not shown).

The incertitude in the location of the ^{23}Na cations in the bare zeolite and the difficulties to interpret the ^{133}Cs MAS NMR spectra prevent us to asseverate if cation migration occurs upon adsorption of pyrrole. Nevertheless, our NMR results strongly suggest that some redistribution of supercage Cs^+ cations must occur upon pyrrole adsorption and that the adsorbed molecules interact with Cs^+ and Na^+ up to a degassing temperature of 423 K.

IR Spectroscopy: The Pyrrole−Framework Interactions. Besides the donation of electronic charge from the ring system of pyrrole to the alkaline cations in the exchanged zeolites, the −NH group forms hydrogen bridges with adjacent basic framework oxygen. In consequence, the N−H bond is polarized, as inferred from the displacements of both infrared stretching band (toward lower frequencies)[5,7] and ^{1}H chemical shift (toward lower fields)[9] dependent on the zeolite basicity. Because of the different time scale between both spectroscopies, ^{1}H NMR chemical shift gives an average basicity of the pyrrole adsorption sites,[9] while the presence of several components in the −NH infrared bands evidences the basic site heterogeneity.[12,14]

The different components of the NH stretching band were attributed to pyrrole interacting with oxygen atoms in the vicinity of the two types of cations[12,14] and, on the basis of known site population, of cations located in supercage, sodalite, and hexagonal prisms.[14] However, our NMR results indicate that upon admission of pyrrole, (i) cation migration occurs, (ii) the adsorption takes place over cations located in the supercage, and (iii) at low coverages, preferential adsorption over more electropositive cations occurs in partially exchanged zeolites. These results strongly suggest that the local basic strength must be governed by factors other than the type of alkaline cations and their distribution.

The basicity of alkali-exchanged zeolites of type FAU has been studied by Density Functional Theory (DFT) methods, using clusters of four and six rings interacting with an alkaline cation to model the framework topology.[50] The calculations indicated that the basic character of the oxygen is dictated by the number of aluminum atoms and its relative position in the ring, whereas smaller effects are observed by the exchange of Na^+ by K^+.[50] On the other hand, our solid-state NMR results suggest that one pyrrole molecule interacts with one alkaline cation in the supercage, supporting the model proposed for the adsorption of pyrrole on NaY from theoretical calculations.[16,17] Assuming this model, which allocates the Na^+−pyrrole complex at the SII positions, the six-ring composition (and the distribution of the T atoms in it) will determine the basicity of the oxygen and thus the −NH stretching frequency of the adsorbed pyrrole.

According to this hypothesis, we interpret the infrared spectra assuming that pyrrole binds to cations at sites SII and that the −NH frequency mainly depends on the number of Al atoms at the six ring. However, the cations forming complexes with pyrrole might occupy other supercage positions (probably SIII or SIII') and therefore be in a different coordination environment. This must be the case for zeolites NaY and KNaY at high coverage (degassing temperature of 338 and 393 K in the NMR experiment), as the number of adsorbed pyrrole molecules is higher than the number of SII sites. Nevertheless, we believe that the model involving the interaction with the cations located at sites SII is valid for the adsorption of pyrrole over alkali-exchanged zeolites Y at low pyrrole contents. The spectra are analyzed on the basis of the NMR results, assuming no changes in the extinction coefficients of the −NH band of pyrrole. Although the experimental conditions to record the FTIR and the NMR spectra are not identical, the samples are submitted to similar treatments, and we are convinced that the main adsorption features are preserved. For every zeolite, we have simulated the −NH band at low coverage first, when pyrrole selectively interacts with the more electropositive cation.

The infrared spectra of adsorbed pyrrole consist of very broad −NH stretching bands between c.a. 3200 and 3450 cm^{-1}, a series of narrow bands including the C−H stretching modes in the range 3100−2500 cm^{-1}, and another series in the ring-stretching region 1300−1500 cm^{-1} (not shown). The assignment of the infrared spectra has been extensively discussed,[5,7,12,17] and we shall only consider the −NH stretching bands. Figures 8−11 show this region for the alkali-exchanged zeolites Y after the adsorption of pyrrole at room temperature and subsequent degassing in the temperature range 338−423 K. The spectra shown in the figures have been normalized.

All the spectra show the presence of several components (see Figures 8−11), in agreement with literature data.[5,12,14] For all samples, the relative intensity of the low-frequency components progressively increases as the degassing temperature increases,

(50) Vayssilov, G. N.; Rösch, N. *J. Catal.* **1999**, *186*, 423.

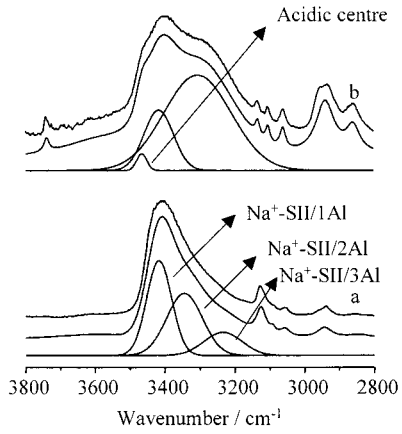

Figure 8. FTIR spectra of pyrrole adsorbed on zeolite NaY at room temperature and subsequent degassing at (a) 338 K and (b) 423 K. The intensity of the spectra is normalized.

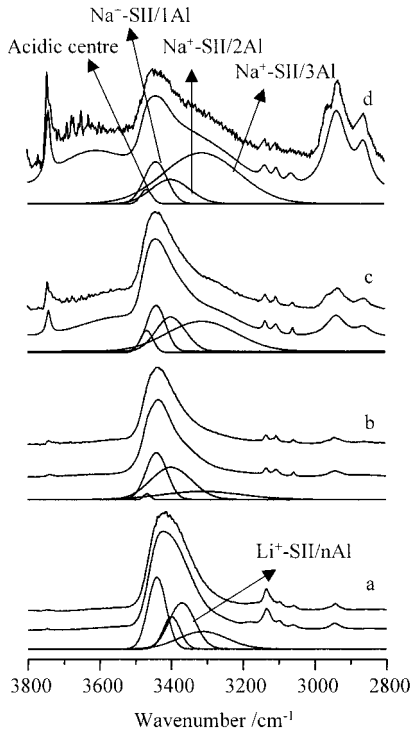

Figure 9. FTIR spectra of pyrrole adsorbed on zeolite LiNaY at room temperature and subsequent degassing at (a) 338 K, (b) 393 K, (c) 423 K, and (d) 473 K. The intensity of the spectra is normalized.

indicating that pyrrole is adsorbed over more basic centers as the loading decreases. Table 5 shows the results of the decomposition and the mean −NH stretching frequency calculated for all samples, which shifts to lower frequency as the basicity of the sample increases.[9] The same trend is observed when the desorption temperature is increased, indicating a higher average basicity of the adsorption sites.

Figure 8 shows the infrared spectra of pyrrole adsorbed on zeolite NaY and the results of the simulation. After degassing at 473 K, the spectrum can be decomposed in two bands centered at 3416 and 3305 cm^{-1} assigned to pyrrole molecules adsorbed over basic sites and in a third component at 3465 cm^{-1}. The latter appears at higher frequency than physisorbed pyrrole (3415 cm^{-1})[12] and can be assigned to species adsorbed over acidic centers.[12,13,14] The spectrum obtained after degassing at 338 K can be simulated with the two low-frequency components,

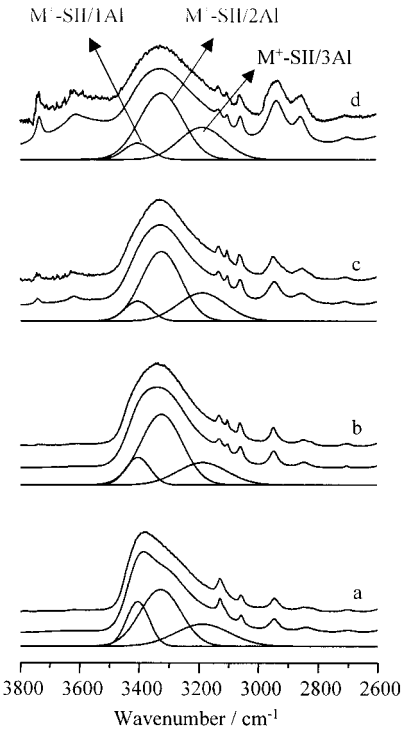

Figure 10. FTIR spectra of pyrrole adsorbed on zeolite KNaY at room temperature and subsequent degassing at (a) 338 K, (b) 393 K, (c) 423 K, and (d) 473 K. The intensity of the spectra is normalized.

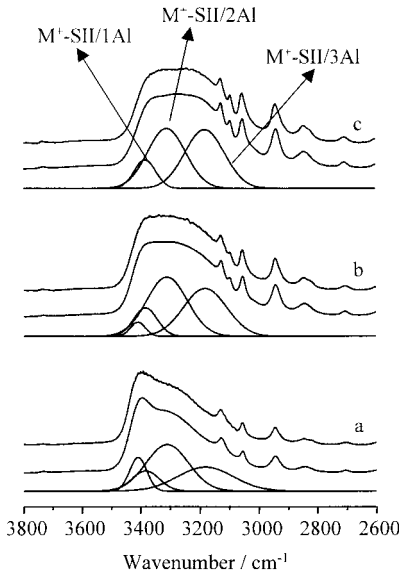

Figure 11. FTIR spectra of pyrrole adsorbed on zeolite CsNaY at room temperature and subsequent degassing at (a) 338 K, (b) 393 K, and (c) 423 K. The intensity of the spectra is normalized.

but the result is improved by decomposing the band at 3305 cm^{-1} in two at 3344 and 3234 cm^{-1}. According to our model, the three infrared bands at 3416, 3344, and 3234 cm^{-1} can be assigned to the −NH group of pyrrole adsorbed on a Na^+ SII site forming hydrogen bonds with oxygen atoms in six-member rings containing one, two, and three aluminum atoms, respectively. Theoretical calculations show that the oxygen atoms in the six ring with the two Al in meta positions are slightly more basic than those in rings containing three Al atom,[50,51] and

(51) Vayssilov, G. N.; Lercher, J. A.; Rösch, N. *J. Phys. Chem. B* **2000**, *104*, 8614.

Table 5. Results of the Simulation of the Infrared Spectra of Pyrrole Adsorbed on Alkali-Exchanged Zeolites Y Dehydrated at 673 K[a]

		intensity of the NH stretching band (%)					
zeolite	T_d (K)	SII/1Al	SII/2Al	SII/3Al	other	Si/Al_{ap}[b]	ν_{NH}[c]
		3440 cm^{-1}[d]	3399 cm^{-1}[d]	3312 cm^{-1}[d]	3370 cm^{-1}[d]		
LiNaY	338	33.6	14	21.9	30.5	2.28	3384.9
					3467 cm^{-1}		
	393	33.1	43.9	21.9	1.3	2.18	3394.5
	423	20.4	43.9	49.1	6.6	1.60	3369.2
	473	16.4	15.9	65.2	2.6	1.40	3350.9
		3416 cm^{-1}[d]	3344 cm^{-1}[d]	3234 cm^{-1}[d]	3465 cm^{-1}[d]		
NaY	338	43.3	40.6	16.1			3357.7
	423	14.9	63.8	19.1	2.2	1.94	3336.5
		3404 cm^{-1}	3329 cm^{-1}	3208 cm^{-1}			
KNaY	338	20.4	37.3	27.0			3308.6
	393	11.1	47.9	28.2		1.73	3299.5
	423	8.5	38.8	27.7		1.66	3292.9
	473	6.3	24.4	21.2		1.62	3288.7
		3384 cm^{-1}	3310 cm^{-1}	3180 cm^{-1}	3409 cm^{-1}[d]		
CsNaY	338	30.1	12.5	44.2	13.1	1.93	3293.5
	393	38.6	12.5	45	3.9	1.70	3273.3
	423	40.6	8.8	50.7		1.59	3264.2

[a] The vapor pressure of pyrrole was adsorbed at room temperature and subsequently desorbed at increasing temperature. The underlined figures indicate the frequency positions of the components resulting from the decomposition of the −NH stretching bands. [b] Apparent Si/Al ratio calculated as $Si/Al_{ap} = [\sum_{n=1}^{n=3}(6-n)I_{SII/nAl}]/[\sum_{n=1}^{n=3}nI_{SII/nAl}]$, where $I_{SII/nAl}$ is the relative intensity of the −NH infrared band attributed to SII/*n*Al species. [c] Average value of the −NH stretching frequency (cm^{-1}). It is calculated from the results of simulation considering the relative intensity of the components. [d] Adsorption sites associated with Na^+ cations.

therefore should give −NH bands at lower frequency. However, our assignment is based on the results reported for zeolite X. The higher intensity of the lower frequency components when pyrrole is adsorbed over this zeolite, richer in aluminum, must be due to the higher population of the six ring containing three Al atoms.[52] Hereafter, the bands are denoted as M^+-SII/nAl, with $M^+ = Li^+$, Na^+, K^+, or Cs^+, and $n = 1$, 2, or 3. The adsorption sites involving six-member rings without aluminum atoms can be ignored because of its low concentration (c.a. 8%)[52] and weak basicity. For comparative purposes, we have simulated the spectrum recorded after degassing at 423 K using three −NH components. The results of the decomposition, as well as the intermediate −NH frequency are summarized in Table 5.

Figure 9 shows the results obtained on the adsorption of pyrrole over the zeolite LiNaY by infrared spectroscopy. The spectra recorded after degassing the pyrrole in the temperature range 393−473 K can be simulated using three bands at 3440, 3399, and 3312 cm^{-1} and a weak peak at 3467 cm^{-1} of pyrrole adsorbed over acid centers. The results are depicted in Figure 9d and Table 5. According to the NMR data, after degassing over 338 K, pyrrole is selectively adsorbed over sites involving Na^+ cations. Therefore, the three low-frequency components at 3440, 3399, and 3312 cm^{-1} can be attributed to pyrrole adsorbed over Na^+−SII/1Al, Na^+−SII/2Al, and Na^+−SII/3Al sites, respectively. The spectrum obtained after degassing at 338 K cannot be simulated in the same way as the spectra 9 b−d, and a new band at 3370 cm^{-1} must be added. In some way, this band must represent the pyrrole molecules adsorbed over sites involving Li^+ cations at higher loadings. Although the band frequency (3370 cm^{-1}) is low, this interpretation is supported by the agreement between the relative contribution of this band (30%) and of affected Li^+ (30% of the total number of cations) as deduced from NMR. Then, the mean −NH frequency calculated after degassing at 338 K is lower than that at 393 K, which does not agree with the general trend that pyrrole is adsorbed over more basic sites at lower contents. This can be tentatively explained by considering that sites SII are not fully occupied in zeolite LiNaY[38] and therefore that Li^+ cations will probably occupy SII sites compensating six-member rings richer in Al than the average bulk zeolite composition.

The −NH stretching bands assigned to pyrrole interacting with oxygen atoms at Na^+−SII/(1−3)Al sites are shifted to higher frequency for zeolite LiNaY than for NaY, suggesting that the local basicity of the adsorption site is also affected by the nature of the cations in its vicinity or by the average zeolite basicity.

The results obtained by the simulation of the infrared spectra of pyrrole adsorbed over zeolite KNaY are represented in Figure 10 and are summarized in Table 5. The NMR results evidence the interaction of pyrrole with both Na^+ and K^+ in the whole range of degassing temperatures studied here. Since the simulation of the infrared spectra with all possible contributions makes no sense, we have used only three bands at 3404, 3329, and 3208 cm^{-1} which are assigned to pyrrole on adsorption sites associated either to K^+ or Na^+ in six-member rings containing one, two, or three aluminum atoms, respectively. A similar approach was adopted to analyze the spectra of pyrrole adsorbed on zeolite CsNaY as shown in Figure 11 and Table 5. The main difference is that the bands appear shifted to lower frequency than those used for zeolite KNaY. Moreover, a fourth peak at 3409 cm^{-1} is required to obtain a good fit of the spectrum recorded after degassing the pyrrole at 338 and 393 K. The position of this band suggests its attribution to pyrrole bonded to Na^+ located at SII sites in ring with 1 Al atom by comparison with the results obtained for zeolite NaY (see Table 5). The relative intensity of this component increases when pyrrole is adsorbed on less basic centers at higher loading.

(52) Klinowski, J.; Ramdas, S.; Thomas, J. M. *J. Chem. Soc., Faraday Trans. 2* **1982**, *78*, 1025. Melchior, M. T.; Vaughan, D. E. W.; Jacobson, A. J. *J. Am. Chem. Soc.* **1982**, *104*, 4859.

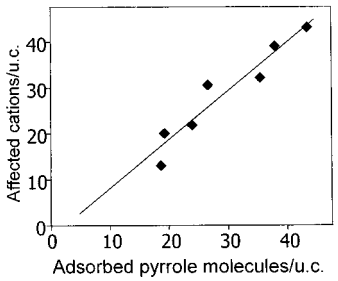

Figure 12. Correlation between the number of adsorbed pyrrole molecules as determined by ^{1}H MAS NMR and the number of interacting cations estimated from the relative intensity in the corresponding MAS NMR spectra.

Discussion

The interaction of guest molecules with alkali-exchanged zeolites provokes dramatic changes in the NMR spectra of the compensating cations. The modifications observed for those occupying accessible sites are explained by the binding to supercage molecules.[9,23,24,31] The changes experienced by cations at nonaccessible SI' positions in the bare zeolite are explained by their migration to the supercage, in agreement with previously reported results for the adsorption of hydrofluorocarbon molecules on zeolite NaY[23,24] Further evidence of the displacement of the cations is reported here by ^{7}Li MAS NMR of zeolite LiNaY. The appearance of a signal shifted to low frequency at high pyrrole contents indicates the direct interaction of the cation (Li^+) with the π system of the pyrrole ring.[9,44] As Li^+ at SII sites are not accessible to the supercage molecules, the interaction with pyrrole requires the displacement of the cation from its original position in the bare zeolite.[35−38] The results shown here prove that the adsorption of pyrrole over alkali-exchanged zeolites Y induces a redistribution of the cations to an extent that depends on the loading. In general, we observe that cations within the sodalite units or at SII sites shielded by the framework oxygen are able to move toward the supercage and bind the adsorbate molecules. From our results, it is not possible, however, to ascertain if other migrations processes involving less populated sites occur.

The shift observed on the ^{7}Li MAS NMR spectra of the LiNaY zeolite was taken by ourselves as evidence of the formation of a Li^+−pyrrole complex by the donation of electron density from the heterocycle of pyrrole.[9] Moreover, as shown in Figure 12, there is a good agreement between the number of adsorbed molecules and the number of affected cations for zeolites LiNaY, NaY, and CsNaY at different pyrrole content (the data for zeolite KNaY have not been included because the number of K^+ cations interacting with the adsorbate was not determined). These experimental results support the adsorption model proposed from theoretical calculations for zeolite NaY, in which one molecule is adsorbed on one Na^+ occupying an SII site, and makes it extensive to other alkali-exchanged zeolites Y. Although from our results it is not possible to locate the cation−pyrrole complexes formed at specific supercage sites, we assume the adsorption site proposed previously[16] as it is compatible with our results. Only the large amount of pyrrole remaining after degassing at 338 K the zeolite NaY (and KNaY), approximately the same as the number of affected cations, suggests that some Na^+−pyrrole complexes must be located in supercage positions other than SII.

The NMR results presented here clearly indicate that pyrrole is selectively adsorbed over more electropositive cations. In bare alkali-exchanged zeolites, the Lewis acidity of the alkaline cations decreases from Li^+ to Cs^+, which can be rationalized in terms of acid−base pairs: the more electropositive cation will have a weaker acidic character and the stronger will have the conjugated basis, that is, the basic oxygen atoms.[5] Therefore, a weaker interaction of the more eletropositive cations with the zeolite framework will favor its bonding to the pyrrole molecules. Moreover, bulkier cations are usually occupying more accessible positions in the supercage and therefore the cationic migration is not so demanding at low loading. Besides this, also the hydrogen bonding of the −NH group with the framework oxygen has to be considered, which as shown by IR, is stronger with the sites involving more voluminous cations, possessing a higher local basicity. This latter observation is in agreement with the general trend observed for the zeolites when the nature of the alkaline cation is varied. The interaction of pyrrole with both the cation and the basic framework oxygen atoms is favored on the same type of centers. Therefore, as already suggested in the former work,[5] the conjugated acid−base pair formed by the cation and the framework oxygen atoms has to be considered to rationalize the adsorption of pyrrole on alkali zeolites.

Another aspect to be considered when studying the adsorption of pyrrole on alkali zeolites is the origin of the basicity heterogenetity evidenced by infrared spectroscopy. The combination of the NMR and IR results indicates that for a given zeolite, adsorption sites containing the same type of cation occupying similar positions possess different basic strength, and then, that other factors must determine the local basicity. We have assumed that the oxygen basicity increases with the number of Al atoms in the six-member rings of the SII sites. With this hypothesis and the results derived from the simulation of the spectra, we have calculated what we call the apparent Si/Al ratio Si/Al_{ap}. As shown in Table 5, when the loading decreases, the relative population of pyrrole interacting with more basic oxygen in rings with more aluminum atoms increases, and the Si/Al_{ap} decreases. Therefore, the comparison with the Si/Al framework ratio gives an idea on the preferential adsorption over more basic sites. We also observe that the stretching frequency of bands assigned to pyrrole adsorbed on a specific type of site depends on the zeolite host. This can be explained by considering that the local basicity of an adsorption site is also affected by the overall zeolite basicity or by the nature of the nearby cations.

One open question is the driving force on the adsorption of pyrrole: the electrostatic interaction with the cation or the hydrogen bonding with the basic framework oxygen. In any case, the adsorption site should be properly described as an acid−base conjugated pair. This picture immediately leads to question the validity of the use of pyrrole as a probe to characterize the zeolite basicity, moreover, when the alkali cations redistribute upon the adsorption. It is true that the migration processes will strongly depend on the nature of the adsorbate or of the reactants and products. However, the use of pyrrole gives valuable information since many adsorptions and reactions proceed on acid−base conjugated centers.

Conclusions

In this work, the combined use of solid-state NMR and infrared spectroscopy has allowed a deeper insight on the species

formed upon the adsorption of pyrrole on alkali-exchanged zeolite Y and on the nature of the host−guest interactions. The ^{23}Na, ^{7}Li, and ^{133}Cs MAS NMR spectra of alkali-exchanged zeolite Y changes with the pyrrole loadings. The decrease on the QCC value of ^{23}Na and the appearance of high field shifted signals of ^{7}Li and ^{133}Cs are ascribed to the formation of cation−pyrrole complexes by donation of electron charge density from the π ring system of pyrrole. The quantitative analysis of the ^{1}H NMR spectra in combination with the NMR results of the alkali cations strongly suggest that one pyrrole molecule interacts with one cation. The adsorption of pyrrole provokes a redistribution of the cations to an extent dependent on the loading. Although our results do not allow to assert the position of the supercage cation bonded to pyrrole, they are consistent with their location at SII sites. Moreover, when the amount of adsorbed pyrrole decreases, it is selectively adsorbed over more basic sites, containing more electropositive cations.

In this way, at high pyrrole contents (degassing temperature of 338 K), Na^+ in zeolites NaY and LiNaY migrate from the sodalite SI' sites toward the supercage to reach a stoichiometry of 1:1 in the cation−pyrrole interaction. In this latter zeolite, the formation of Li^+−pyrrole complexes only occurs after desorbing at 338 K. Since Li^+ cations at the SII sites are screened by the framework oxygen atoms, they must displace from their original position to bind the adsorbate molecules. The sum of Na^+ and Li^+ cations affected by adsorbed pyrrole is again in good agreement with the number of pyrrole molecules present. When the degassing temperature increases and the amount of adsorbed pyrrole decreases, only the interaction with Na^+ is observed. The same trends (cation−pyrrole stoichiometry or 1:1 and preference for adsorption over sites compensating by more electropositive cations) seem to take place on the pyrrole adsorption over zeolites KNaY and CsNaY, although we could not give so clear evidence in these cases because no K^+ nuclei was studied and because of the complications in the interpretation of ^{133}Cs spectra.

With the support of our experimental results, we assume the model previously proposed on the basis of theoretical calculation for NaY[16,17] and make it extensive to other alkali-exchanged zeolites: the ring of pyrrole interacts with the cation located at SII site forming hydrogen bonds with a basic framework oxygen in the six-member ring. On this basis and in consistency with our NMR results, we ascribe the basic site heterogeneity observed by infrared spectroscopy to the presence of six-member rings containing different number of aluminum atoms. We make an assignment of the several components in the −NH infrared bands to pyrrole adsorbed on sites containing alkaline cation in a SII site with the proton of the −NH group pointing to an oxygen of the a six-member ring containing one, two, or three aluminum atoms. The basicity of the center increases with the number of aluminum atoms in the ring, shifting the −NH stretching band to low frequency, and becomes relatively more intense when the number of adsorbed molecules decreases.

Acknowledgment. Financial support by the CICYT (project MAT2000-1392) is gratefully acknowledged.

JA011912J